Polarized x-ray emission studies of methyl chloride and the chlorofluoromethanes

D. W. Lindle, P. L. Cowan, T. Jach, R. E. LaVilla, and R. D. Deslattes
National Institute of Standards and Technology, Gaithersburg, Maryland 20899

R. C. C. Perera
Advanced Light Source, Accelerator and Fusion Research Division, Lawrence Berkeley Laboratory, Berkeley, California 94720

(Received 12 September 1990)

A new technique sensitive to molecular orientation and geometry, and based on measuring the polarization of x-ray emission, has been applied to the Cl-containing molecules methyl chloride (CH_3Cl) and the chlorofluoromethanes (CF_3Cl, CF_2Cl_2, and $CFCl_3$) in the gas phase. Upon selective excitation using monochromatic synchrotron radiation in the Cl K-edge (Cl 1s) near-threshold region, polarization-selective x-ray emission studies reveal highly polarized molecular *valence* x-ray fluorescence for all four molecules. The degree *and* the orientation of the polarized emission are observed to be sensitive to the incident excitation energy near the Cl K edge. In some cases, the polarization direction for x-ray emission reverses for small changes in incident excitation energy (a few eV). It is shown that the polarized x-ray emission technique can be used to infer, directly from experiment, symmetries of occupied and unoccupied valence molecular orbitals, anisotropies in absorption and emission, and orientational and geometrical information. It is suggested that the x-ray polarized-fluorescence phenomenon, reported here for simple molecules, can be used as a new approach to study more complicated systems in a variety of environments.

I. INTRODUCTION

X-ray-emission spectroscopy (XES) has a proven history of elucidating core-level phenomena in atoms, molecules, and solids under a wide variety of conditions.[1,2] Traditionally, this work has relied upon incident excitation by x rays, either from fixed-wavelength sources or polychromatic (Bremsstrahlung radiation) sources, or by high-energy electron impact. These methods have yielded many excellent results.[1,2] However, one desirable goal, namely the ability to selectively excite near-edge features,[3] has remained generally difficult to achieve. This difficulty stems from either the lack of excitation-energy selectivity or the lack of sufficient x-ray intensity of the traditional excitation sources.

Synchrotron-radiation (SR) sources in the x-ray energy range have shown promise in alleviating this difficulty, in particular, providing sufficiently intense tunable (and polarized) x rays throughout the near-threshold regions of the core levels of most elements.[4] The first x-ray-emission measurement of this sort, for the Ar K edge,[5] illustrated the soundness of this approach, and revealed a wealth of information on resonant and multivacancy effects in x-ray spectra not previously attainable. Since that initial experiment, a SR beamline dedicated to XES has been commissioned,[6] and preliminary results have been reported.[7–13] The critical importance[3] of selective excitation by tunable incident radiation has been borne out by these new results.

Among this small body of near-threshold XES results, one type of experiment[9–12] to which this report is addressed combines the advantages of monochromatic SR (tunability, polarized excitation) with polarization analysis of the x-ray fluorescence. The initial polarized x-ray-emission spectroscopy (PXES) measurements were performed near the Cl K edge of the gas-phase molecule methyl chloride, CH_3Cl, and showed that large changes in the degree of fluorescence polarization could be induced by carefully selecting the incident energy in the near-threshold region. A straightforward theoretical interpretation[10,14] applied to the CH_3Cl measurements revealed that the anisotropy of the photoexcitation process and the orientations and relative magnitudes of fluorescence dipole transition moments are obtainable directly from experiment.

It is important to note that the measurements described herein and in Refs. 9–12 pertain to randomly oriented samples in the gas phase. A considerable body of previous work[15–21] has already shown that polarized x-ray emission is observable from crystalline samples, such as MoS_2 (Mo L edge) and GaS (S K edge) (Refs. 16 and 17, respectively). These observations can be understood as due to the aligned nature of the molecular moieties in the crystalline samples. Indeed, explanations and calculations based on this principle have been put forth with success.[16–23] Small emission-polarization effects also have been measured in atomic Hg following $2p$-subshell ionization.[24] These results, at the ten-percent level, reflect the non-s-subshell (i.e., $l \neq 0$) character of the ionization process and the importance of spin-orbit and relativistic effects in this high-Z atom. In contrast to solid[15–23] and atomic[24] PXES measurements, the molecular results discussed here show more pronounced effects due to alignment produced by selective near-threshold

excitation.

Another related body of work[25] uses polarized visible and ultraviolet (uv) emission to study alignment effects in gas-phase molecular ions and fragments following polarized excitation of *valence* electrons. This type of study differs from PXES in two fundamental aspects. Firstly, core-level holes studied with PXES undergo rapid Auger decay processes ($\approx 10^{-14}$ s), forcing the x-ray emission to occur on a time scale much shorter than normal molecular tumbling periods (10^{-11}–10^{-12} s). In contrast, valence-shell hole states are relatively long lived ($\geq 10^{-10}$ s). Thus, PXES has the advantage that any alignment produced by the absorption process is retained up to the time of fluorescence decay. For visible and uv emission, full retention of alignment is not the case, and indeed complications due to molecular tumbling (and vibrations) must be considered[25] in the interpretation of valence polarized-fluorescence measurements. (Vibrational motion, which may have periods approaching core-hole lifetimes, is discussed further in Sec. III A 1.)

Secondly, PXES is inherently atom specific because individual atomic species can be distinguished easily by their core-level edges. Furthermore, core-level excitation acts as a localized probe of the molecule, simplifying the spectroscopic interpretation of PXES results by effectively eliminating some possible x-ray-emission channels. Valence excitation or ionization, followed by visible or uv fluorescence, involve only electrons in diffuse valence molecular orbitals (MO's), and thus provides a nonlocal, non-atom-specific probe. Finally, a third advantage of x rays, not mentioned in our initial reports,[9–12] is considerable depth of penetration into most materials, possibly permitting studies of dilute solutions, buried interfaces, etc.

To further illustrate the PXES technique, we report here additional results on CH_3Cl and CF_3Cl and new results on CF_2Cl_2 and $CFCl_3$. Polarized x-ray emission is observed at selected incident energies in the Cl 1*s* near-threshold region for all four molecules. Both the degree and direction of the polarization is observed to change with the excitation energy and with the symmetry of the occupied valence MO involved in the emission process. In CH_3Cl, for which the most complete results are available, the spectroscopic usefulness of PXES is illustrated by studying an above-threshold absorption feature, and in so doing directly determining the symmetry of the excitation process associated with that feature.

The experimental details are described in Sec. II. The results for each molecule are presented in turn in Sec. III, and concluding remarks are contained in Sec. IV.

II. EXPERIMENT

Core-level polarized x-ray-emission measurements require (i) an intense source of x rays, (ii) an efficient, high-resolution primary monochromator, (iii) an efficient, high-resolution secondary x-ray spectrometer, and (iv) polarization sensitivity of the secondary spectrometer. In addition, highly polarized incident radiation is desired because it enhances effects observed by PXES. For the present experiment (see Fig. 1), x rays from the National Synchrotron Light Source (NSLS) and energy selected by the National Institute of Standards and Technology (NIST) beamline X-24A equipped with a large-aperture double-crystal primary monochromator were used. The novel design of this primary monochromator, which yields both high throughput and high resolution, has been described in detail elsewhere,[6] so only a few pertinent comments are in order. For the Cl *K*-edge work at ≈ 2.8 keV, Si(111) crystals were used in the primary monochromator, providing a bandwidth of 0.4 eV for all of the present measurements. An added benefit of using Si(111) crystals in the Cl *K*-edge region is that the first-order Bragg diffraction angle is approximately 45°, enhancing significantly the inherent linear polarization of the SR. We estimate that the monochromatic x-ray beam focused onto the gas sample is $\geq 99\%$ linearly polarized. The samples were contained in a 7-mm-long gas cell with 0.025-mm-thick Be windows at pressures of 300, 200, 100, and 60 Torr, respectively, for CH_3Cl, CF_3Cl, CF_2Cl_2, and $CFCl_3$. The primary monochromatic beam passes through ionization chambers, before and after the sample cell, which monitor incident and transmitted fluxes, thereby determining relative photoabsorption cross sections as a function of photon energy for each sample.

The incident beam direction and polarization vector lie in the horizontal plane for the PXES measurements. X-ray fluorescence emitted normal to this plane by excited or ionized molecules passes upward into the secondary spectrometer[26] for energy analysis. The secondary spectrometer is of a Johann geometry, with the dispersing crystal and x-ray detector on a Rowland circle of variable radius, but with the crystal-to-detector distance fixed at nominally 1 m. The sample cell is situated inside the Rowland circle to better utilize the diffuse nature of the gaseous source of the x-ray fluorescence and to reduce sensitivity to alignment of the primary beam with respect to the secondary spectrometer.[27] As in the primary monochromator, a Si(111) crystal is used to diffract the x rays. This crystal is cylindrically curved by a crystal-bending device,[28] and the radius is adjusted externally to optimize the focus (≈ 0.3 mm) and thus the energy resolution (≈ 0.9 eV) for Cl *K* emission. The diffracted x rays are detected by a one-dimensional position-sensitive proportional counter (PSPC) that has been described previously.[29] Operation with the PSPC allows a complete x-ray-emission spectrum (≈ 40-eV-wide window at the Cl *K* edge) to be accumulated simultaneously.

One drawback to this geometry is that each x-ray-emission peak detected in the PSPC receives contributions from x rays which traverse slightly different paths from the gas cell to the crystal and then to the detector. Thus, it is possible that intensity changes in the x-ray spectra may occur due to variations in the source brightness with position, or irregularities in the diffracting crystal or the detector. Of course, this problem is worse if the sample cell is placed on the Rowland circle, for which point-to-point focusing from the sample to the detector would occur. With the sample cell well inside the Rowland circle, this issue is mitigated because the entire source region, rather than a single point in it, contributes

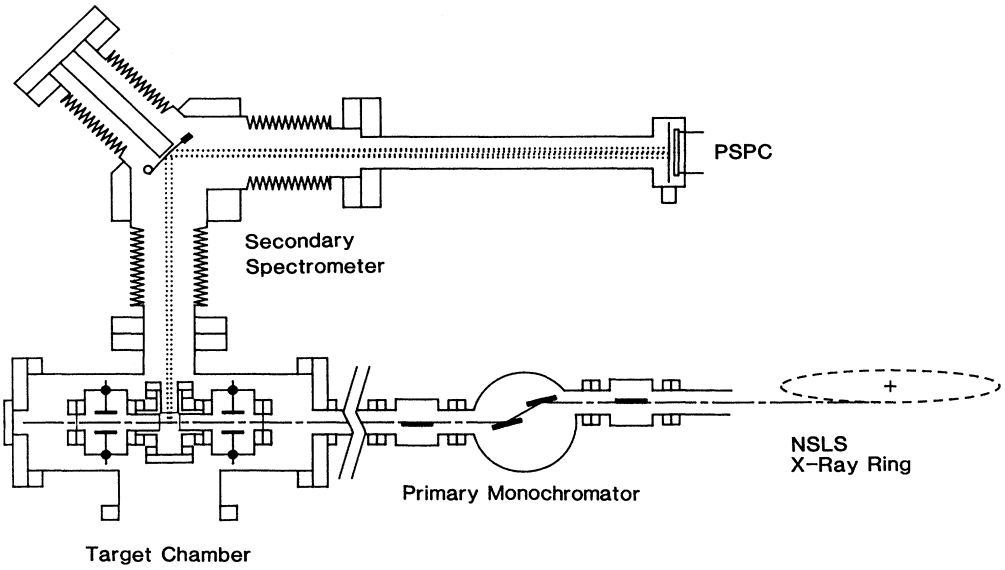

FIG. 1. Schematic representation of the polarized x-ray-emission spectroscopy (PXES) experiment. Synchrotron radiation is provided by the x-ray ring at the NSLS, energy selected by a double-crystal monochromator, and focused into a cell containing the sample. The secondary spectrometer analyzes the x-ray emission as described in the text. (PSPC=position-sensitive proportional counter.)

to each emission peak. Anyway, potential problems of this sort have been checked by varying the gas pressure, beam profile and intensity, the overall position of the source (excited sample) with respect to the secondary spectrometer, and the radius of the Rowland circle. No discernible effects have been observed under normal variations in operating conditions and geometry. Overall resolution of the secondary spectrometer is 0.9 eV for the present experiments, which is attributed primarily to the PSPC. The absolute efficiency of the secondary spectrometer has been determined to be 7×10^{-7} using a calibrated Fe 55 radioactive source, where this value naturally includes a factor for the solid angle subtended by the crystal relative to 4π sr. The efficiency should be somewhat better for Cl K-edge emission due to a larger crystal profile for larger Bragg angles.

Polarization selectivity of the secondary spectrometer to Cl K-edge fluorescence ($\approx$2.8 keV) is provided by the use of a Si(111) crystal at a Bragg angle of 44.6°. The polarization component of the x-ray fluorescence to be measured (parallel to the crystal surface) is thus diffracted more efficiently by at least a factor of 10^3 relative to the orthogonal component (out of the plane of the crystal surface). Polarization selection is accomplished simply by orienting the dispersion plane of the secondary spectrometer either parallel (as in Fig. 1) or perpendicular to the propagation vector of the SR, ensuring that fluorescence from the sample polarized parallel or perpendicular, respectively, to the incident polarization vector is primarily detected. Thus, a rotation of the secondary spectrometer by 90° about the vertical axis of Fig. 1 suffices to measure orthogonal polarizations of x-ray emission.

With the apparatus as described, approximately 10^{11} photons/s in a 0.4-eV bandpass are delivered to the sample. The subsequent valence-electron K-V x-ray emission is accumulated at $1-10\ s^{-1}$, depending on the experimental conditions. Most spectra were accumulated for 30–60 min.

III. RESULTS

In this section, each molecule studied will be discussed in turn. For the CH_3Cl and CF_3Cl results, previous publications[10–12] should be consulted for some additional details and discussion.

A. CH_3Cl

Figure 2 shows a measured absorption spectrum of CH_3Cl in the vicinity of the Cl K edge and a Cl K-V (historically referred to as $K\beta$)[30] valence-electron fluorescence spectrum taken with an incident photon energy of 2880 eV, well above the Cl 1s threshold. Peak labels have been adopted from Refs. 31 and 32. Peak energies are listed in Table I, along with results from previous work.[32–35] Peak assignments are from Ref. 10. Overall, the general appearance and peak positions in both absorption and emission agree well with earlier results.[2,31–38] The present assignments are consistent with previous ones[35,38] based on Cl K-edge work, with measurements in other core-level regions (C K and Cl L) of the molecule,[39–41] and with valence MO orderings.[42–52] For the absorption spectrum, feature D is of major interest, and is attributed[10] to Cl 1s (CH_3Cl $1a_1$) excitation to the $8a_1$ antibonding MO.

The Cl K-V fluorescence spectrum in Fig. 2 results from electrons in valence MO's filling the Cl(1s) hole produced by absorption of the incident radiation. The rela-

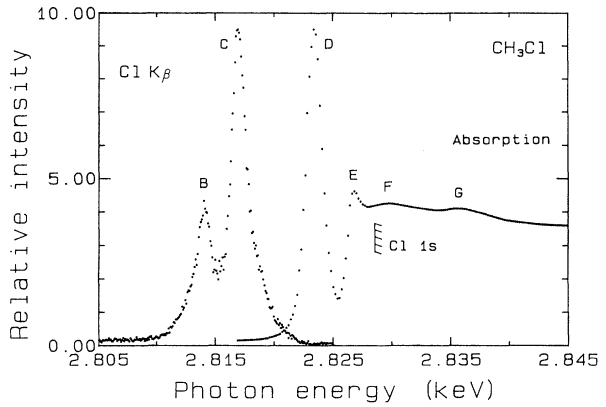

FIG. 2. Cl K absorption spectrum (right) and Cl K-V emission spectrum (left) of CH_3Cl. The emission spectrum was taken with 0.9-eV resolution at an excitation energy of 2880 eV, and exhibits no detectable change with fluorescence polarization angle. Peak labels are adopted from Refs. 31 and 32. The hashed mark represents the Cl 1s ($1a_1$ in CH_3Cl) threshold energy of 2828.4 eV.

tive simplicity of the emission spectrum (i.e., only two peaks) reflects the fact that only MO's with significant atomic Cl 3p character contribute because of dipole selection rules (hence, Cl 3p but not Cl 3s character), and because the K hole is localized on the Cl atom (hence, Cl 3p but not carbon 2p character). The relevant valence MO's (i.e., with Cl 3p character) of CH_3Cl are the three outermost filled orbitals; 3e, $7a_1$, and 2e, in order of increasing binding energy. We observe only two peaks in the K-V fluorescence spectrum because the fluorescence due to the $7a_1$ and 2e orbitals is unresolved in peak B. Finally, we note that there exist contributions on the high-energy side of peak C in Fig. 2 that are attributed to satellite transitions due to multiple-vacancy states produced by photoexcitation at 2880 eV.[32]

The absolute energy scale for Cl K absorption and K-V emission in CH_3Cl (Fig. 2 and the presents results in Table I) was established in the following manner. First, the feature-D energy position in the absorption spectrum was taken as 2823.4 eV.[32] Having fixed this single energy in our absorption spectrum, we used the known properties of Bragg diffraction with a Si(111) crystal (2d spacing of 6.271 Å) (Ref. 53) and the known characteristics of the angle driver of the primary monochromator to determine the dispersion of the absorption spectrum. Inaccuracies introduced in this way for the narrow energy range of Fig. 2 are expected to be quite small. The resulting absolute energies of the CH_3Cl Cl K absorption features are listed in Table I.

Using the established energy scale for the absorption spectrum, determination of Cl K-V emission energies was accomplished by measuring x rays of known energy from the primary monochromator that were elastically scattered from the gas sample into the secondary spectrometer. In this procedure, care was taken to avoid measuring elastic scattering at energies near discrete absorption features in the sample gas. Measuring elastic peaks at several photon energies in the Cl K-edge region thus provided energies of the K-V peaks. The results for the Cl K-V energies in CH_3Cl are included in Table I, along with previous determinations for comparison.[32–35]

The final step in the energy calibration procedure was to determine the Cl(1s) ionization potential (IP). This is easily obtained by summing the K-V x-ray-emission energy and the binding energy for a given valence MO. We use the prominent 3e MO (peak C), because the $7a_1$ and 2e MO's are unresolved. The 3e binding energy is taken from ultraviolet photoelectron spectroscopy (UPS) measurements, and is equal to 11.30 eV.[42–44,46,48,50,54] Thus, we determine the Cl 1s IP to be 2828.4(3) eV for CH_3Cl, in reasonable agreement with previous determinations of 2828.5 eV (Ref. 32) and 2828.7 eV,[34] and with a recent calculation[35] of 2828.8 eV. The hashed mark in Fig. 2 indicates the position of the Cl 1s IP.

TABLE I. Energies and assignments of Cl K-V x-ray emission peaks and Cl-K absorption features of CH_3Cl. The values in parentheses denote errors in the last digit(s).

Peak or feature	Energy (eV) This work	Ref. 32[a]	Ref. 34[b]	Ref. 35[c]	Assignment
B	2814.1(3)	2814.0		2815.2	$7a_1$, $2e \rightarrow 1a_1$
C	2817.1(3)	2817.2	2817.4[d]	2818.2	$3e \rightarrow 1a_1$
D	2823.4[e]	2823.4[e]	2823.1		$1a_1 \rightarrow 8a_1$
E	2826.8(3)	2827.4	2826.6		$1a_1 \rightarrow np$ Rydberg
Cl K IP	2828.4(3)	2828.5	2828.7	2828.8	threshold
F	2829.7(5)	2831			
G	2836(1)	2836			doubly excited state (Ref. 32)

[a]Perera *et al.*
[b]Hanus and Gilberg.
[c]Larkins and Phillips.
[d]Gilberg (Ref. 33).
[e]LaVilla (Ref. 58).

1. Peak D excitation

With 2880-eV excitation, as for the emission spectrum in Fig. 2, no detectable change with fluorescence-polarization angle was observed. Conversely, using near-threshold excitation at 2823.4 eV,[10,12] centered on feature D of the absorption spectrum in Fig. 2, strikingly different K-V spectra are obtained as a function of the emission polarization angle (see Fig. 3). The parallel and perpendicular symbols in Fig. 3 refer to the experimental geometries described in Sec. II and shown in Fig. 1 for the parallel case. In Fig. 3, the relative intensities of peak C have been scaled equally in each spectrum for purposes of comparison. The significant difference in the B-to-C peak ratios in the two orthogonal polarizations is the essential point of this work, and forms the basis for PXES as a technique to study molecules. (Differences between the K-V spectra of Figs. 2 and 3 can be seen also, such as shifts in peak energies, elimination of satellite transitions, and narrowing due to resonant excitation. All of these phenomena have been or will be dealt with in detail in other publications.[5,7,8,13])

Qualitatively, the PXES results of Fig. 3 can be understood by realizing that CH_3Cl molecules excited with incident energies on feature D ($1a_1 \rightarrow 8a_1$) will preferentially have their molecular symmetry axes (along the C—Cl bond) aligned with the direction of the SR polarization. This alignment is retained in the subsequent K-V radiative decay because emission occurs so rapidly ($\approx 10^{-14}$ s) that the molecules remain essentially fixed in space throughout the absorption and emission processes. Consequently, because emission from the $7a_1 \rightarrow 1a_1$ transition, which contributes to K-V peak B (see below and Refs. 10, 12, and 38), is also polarized along the molecular symmetry axis, we expect x rays from this transition to be polarized parallel to the SR polarization. Conversely, emission from the $3e \rightarrow 1a_1$ and $2e \rightarrow 1a_1$ transitions (K-V peaks C and B, respectively) is polarized perpendicular to the molecular symmetry axis and thus produce x rays polarized perpendicular to the SR polarization. This qualitative argument was used in Ref. 10 to rationalize the observation in Fig. 3.

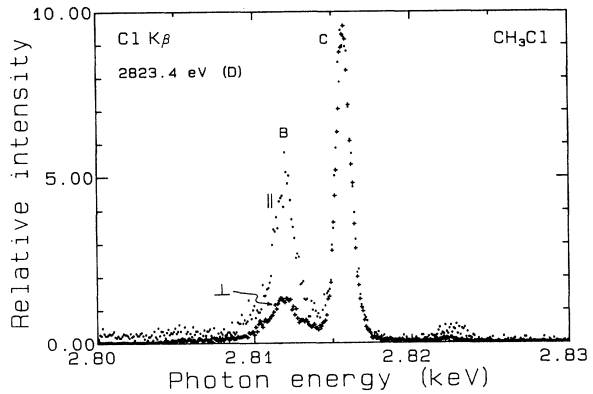

FIG. 3. Cl K-V emission spectra from CH_3Cl following Cl $1s \rightarrow 8a_1$ excitation with 2823.4-eV photon energy, centered on feature D of the absorption spectrum of Fig. 2. The labels parallel and perpendicular refer to orthogonal orientations of the measured fluorescence polarization relative to the incident E vector. The two spectra have been scaled so that the areas of peak C are identical. The peak at 2823.4 eV is due to elastic scattering of the incident radiation.

Quantitative interpretation of the results in Figs. 2 and 3 is based[10] on the following general expression for the emission polarization P valid for C_{3v} symmetry molecules (and linear molecules, also):

$$P=\frac{I_\parallel - I_\perp}{I_\parallel + I_\perp}=\frac{a_\parallel f_\parallel - a_\parallel f_\perp - a_\perp f_\parallel + a_\perp f_\perp}{2a_\parallel f_\parallel + 3a_\parallel f_\perp + 3a_\perp f_\parallel + 7a_\perp f_\perp} , \quad (1)$$

where $I_\parallel$ and $I_\perp$ are integrated relative intensities of K-V emission peaks in parallel or perpendicular polarization, respectively, $a_\parallel$ and $a_\perp$ are body-frame absorption (dipole) transition strengths for incident polarization parallel or perpendicular to the molecular symmetry axis, respectively, and $f_\parallel$ and $f_\perp$ are x-ray-emission transition strengths analogous to $a_\parallel$ and $a_\perp$. The essential qualitative and quantitative features for polarized x-ray-emission presented so far were discussed originally by Gelmukhanov and Mazalov[14] in the context of gas-phase diatomic molecules.

For CH_3Cl, $f_\parallel = 0$ for the $3e \rightarrow 1a_1$ and $2e \rightarrow 1a_1$ transitions, and $f_\perp = 0$ for the $7a_1 \rightarrow 1a_1$ transition. Furthermore, in the case of peak-D excitation, $a_\perp = 0$, yielding $P = -\frac{1}{3}$ for $3e \rightarrow 1a_1$ and $2e \rightarrow 1a_1$, and $P = \frac{1}{2}$ for $7a_1 \rightarrow 1a_1$. Compiling all this information yields[10]

$$\frac{I_{B\parallel}}{I_{C\parallel}}=\frac{(\frac{9}{4})f_\parallel(7a_1 \rightarrow 1a_1)+f_\perp(2e \rightarrow 1a_1)}{f_\perp(3e \rightarrow 1a_1)} , \quad (2a)$$

$$\frac{I_{B\perp}}{I_{C\perp}}=\frac{(\frac{3}{8})f_\parallel(7a_1 \rightarrow 1a_1)+f_\perp(2e \rightarrow 1a_1)}{f_\perp(3e \rightarrow 1a_1)} , \quad (2b)$$

for the B-to-C peak-intensity ratios in parallel and perpendicular polarizations following resonant excitation on feature D. The fractions multiplying $f_\parallel(7a_1 \rightarrow 1a_1)$ in Eqs. (2), i.e., $\frac{9}{4}$ and $\frac{3}{8}$, derive from the resonant-excitation P values for a_1 ($P = \frac{1}{2}$) and e ($P = -\frac{1}{3}$) orbitals, the relation $P = (I_\parallel - I_\perp)/(I_\parallel + I_\perp)$, and the assumption that for peaks in the same x-ray-emission spectrum, peak-intensity ratios depend only on the relative fluorescence transition strengths (the $f_\parallel$ and $f_\perp$ values). For nonresonant excitation far above the Cl K threshold, absorption is believed to be isotropic, no emission polarization is expected, and Eqs. (2) coalesce into

$$\frac{I_B}{I_C}=\frac{f_\parallel(7a_1 \rightarrow 1a_1)+f_\perp(2e \rightarrow 1a_1)}{f_\perp(3e \rightarrow 1a_1)} . \quad (3)$$

In Eqs. (2) and (3), electron multiplicity is implicitly included in the f values.

Equations (2a) and (2b), plus the measured peak intensity ratios of 0.86(5) and 0.34(5) for parallel and perpendicular polarization (Fig. 3), can be used to determine directly the K-V fluorescence yields $f_\parallel(7a_1 \rightarrow 1a_1)$ and $f_\perp(2e \rightarrow 1a_1)$ relative to $f_\perp(3e \rightarrow 1a_1)$. The results are 0.28(4) and 0.24(4) for the $7a_1$ and $2e$ orbitals, respective-

ly. These numbers are somewhat different than those in our preliminary report[10] due to improved analysis of the emission spectra. These new relative transition strengths disagree in magnitude with the calculated values (0.35; 0.11).[10] However, the emission spectra of Figs. 2 and 3 are in good quantitative accord because the sum of the two relative transition strengths [0.52(6)] inferred from Eqs. (2) agrees with that [0.54(5)] obtained directly from the above-threshold K-V spectrum in Fig. 2. This nontrivial result implies that the strengths of the x-ray-emission transitions do not change significantly under different initial excitation conditions. Finally, we also determine that the $7a_1 \rightarrow 1a_1$ transition contributes 54(10)% to the underlying transition strength of emission peak B under conditions of feature-D excitation.

The validity of Eqs. (2) and (3) is critically dependent on the assumption that x-ray-emission peak-intensity ratios depend only on the relative strengths of the contributing transitions. For peaks in the same spectrum, for which Eqs. (2) and (3) are applicable, experimental factors (discussed more below) have been determined to not affect the intensity ratios. However, there are some physical effects which may cause variations in the fluorescence transition strengths f, thereby rendering the measured ratios less indicative of the true relative transition strengths. One factor is the frequency dependence ($\alpha \nu^3$) of the x-ray-emission transition matrix elements. However, for all of the present measurements, this effect is less than 1%, and thus negligible compared to the experimental uncertainty.

A possibly more significant factor affecting the relative x-ray-emission transition strengths has to do with vibrational structure within the absorption and emission processes. For a given emission transition, the Franck-Condon (FC) overlap between the excited K-hole state and the final valence-hole state will depend on the initial absorption process and the valence MO involved in the decay. Different x-ray-emission transitions thus may have quite different FC overlaps with the excited state, affecting their relative strengths. Furthermore, because in general several vibrational levels of the intermediate K-hole state will be accessed, and because the core-hole linewidths are large ($\approx$0.6 eV) compared to the vibrational energy-level spacing ($\approx$0.2 eV), it is possible to have coherent excitation of overlapping vibrational levels in the x-ray-absorption process. This interference effect can lead to significant redistribution of spectral intensity in the decay process, whether radiative[55] or nonradiative.[56] Qualitatively, the interference should be largest when the core-hole lifetime and vibrational frequency are most nearly equal (e.g., at the N and O K edges[55,56]), and when large changes in molecular bond lengths occur during the excitation and emission processes (i.e., when the Born-Oppenheimer approximation is least valid).[56] Only detailed FC and non-FC calculations can reveal the importance of these vibrational effects to the present results, but indications from previous measurements[55,56] suggest that the effects are significantly smaller than the polarization effects observed here for resonant excitation.

So far we have assumed polarization values P for emission peaks B and C upon feature-D excitation based on a classical treatment of the absorption and emission process. However, for peak C at least, it is possible to test directly this assumption using experimental information only. We start with the following expression for the raw measured peak intensity, $N_{\|c}(h\nu)$, for emission peak C in parallel polarization obtained by fitting the PXES spectra:

$$N_{\|c}(h\nu) \propto E_{\|}\sigma_{\text{abs}}(h\nu)pQ(h\nu)I_{\|c}t \ , \tag{4a}$$

$$I_{\|c} \propto f_c \ , \tag{4b}$$

and similarly for perpendicular polarization. In Eqs. (4), $h\nu$ is the incident photon energy, $E_{\|}$ is the secondary-spectrometer efficiency in the parallel-polarization geometry, $\sigma_{\text{abs}}(h\nu)$ is the CH_3Cl absorption cross section, p is the sample density, $Q(h\nu)$ is the incident photon intensity, and t is the data collection time. It is important to properly distinguish among the three quantities $N_{\|c}$, $I_{\|c}$, and f_c. As used in Eqs. (1)–(3), f values refer to *body-frame* transition oscillator strengths (we have dropped the $\|$ and $\perp$ subscripts for simplicity). An f value, properly transformed, yields a *laboratory-frame* transition intensity for a given emission polarization [$I_{\|c}$ in the example of Eqs. (4)]. The use of the symbol $I_{\|c}$ signifies that the I values are to be used in Eq. (1) for quantitative determination of polarization values, P. To obtain *relative* I values, one first measures unnormalized peak intensities (such as $N_{\|c}$), which subsequently can be used with Eq. (4a) to determine I values in a procedure described below.

Now, if we compare two spectra taken under identical experimental conditions, except one is for feature-D excitation and the other is for excitation well-above threshold (2880 eV), we obtain

$$\frac{N_{\|c}(D)}{N_{\|c}(2880)} = \frac{\sigma_{abs}(D)}{\sigma_{abs}(2880)} \frac{Q(D)}{Q(2880)} \frac{I_{\|c}(D)}{I_{\|c}(2880)} \ , \tag{5}$$

where $E_{\|}$, p, and t cancel. The ratio of incident photon intensities, $Q(D)/Q(2880)$ is determined experimentally and is normalized for in a proper manner. Of course, Eq. (5) can be obtained for perpendicular polarization as well. By comparing Eq. (5) for the two polarizations, we find

$$\frac{N_{\perp c}(D)/N_{\perp c}(2880)}{N_{\|c}(D)/N_{\|c}(2880)} = \frac{I_{\perp c}(D)}{I_{\|c}(D)} \frac{I_{\|c}(2880)}{I_{\perp c}(2880)} \ , \tag{6}$$

since the absorption cross section is independent of fluorescence polarization. Based on our observation that parallel and perpendicular spectra well above the Cl(1s) threshold exhibit no polarization effect, we assume that $I_{\|c}(2880) = I_{\perp c}(2880)$. Thus the experimentally determined ratio on the left-hand side of Eq. (6) can be used to determine the ratio of parallel and perpendicular transition intensities for emission peak C following feature-D excitation (or similarly at any other near-threshold energy). This ratio, $I_{\perp}(D)/I_{\|}(D)$, can be used with a modified Eq. (1) to obtain polarization values P. Performing this exercise for K-V peak C for feature-D excitation yields $P_C(D) = -0.32(11)$, which agrees exceptionally well with the theoretical value of exactly $-\frac{1}{3}$. Pictorially, this re-

TABLE II. Measured Cl K-V B-to-C peak-intensity ratios and derived polarization values P for CH_3Cl. Values in parentheses denote errors in the last digit(s).

Photon Energy	B-to-C peak ratio ∥	B-to-C peak ratio ⊥	P_B	P_C	Comments
2822.2	0.75(8)	0.32(3)	−0.01(5)	−0.41(8)	Lt. shldr. of D
2822.8	0.80(8)	0.27(3)	0.22(4)	−0.31(7)	Lt. shldr. of D
2823.4	0.86(8)	0.34(5)	0.11(5)	−0.32(7)	D
2826.8	0.84(8)	0.65(7)	0.10(6)	−0.03(6)	E
2829.2	0.46(5)	0.68(7)	−0.14(6)	0.06(5)	Near F
2829.7	0.56(6)	0.80(8)	−0.04(6)	0.14(5)	F
2830.2	0.58(6)	0.63(6)	−0.02(5)	0.03(6)	Near F
2836	0.56(6)	0.68(7)	−0.10(13)	−0.01(11)	G
2880	0.51(5)	0.57(6)	0[a]	0[a]	

[a]Assumed.

sult indicates that the perpendicular spectrum in Fig. 3 should be multiplied by 1.9(3) for a correct relative comparison between the parallel and perpendicular emission spectra. The exact multiplier would be 2.0 in theory.

2. *Other incident energies*

The primary measured result from the PXES experiment on CH_3Cl is B-to-C peak-intensity ratios at a given incident energy and a given emission polarization angle.

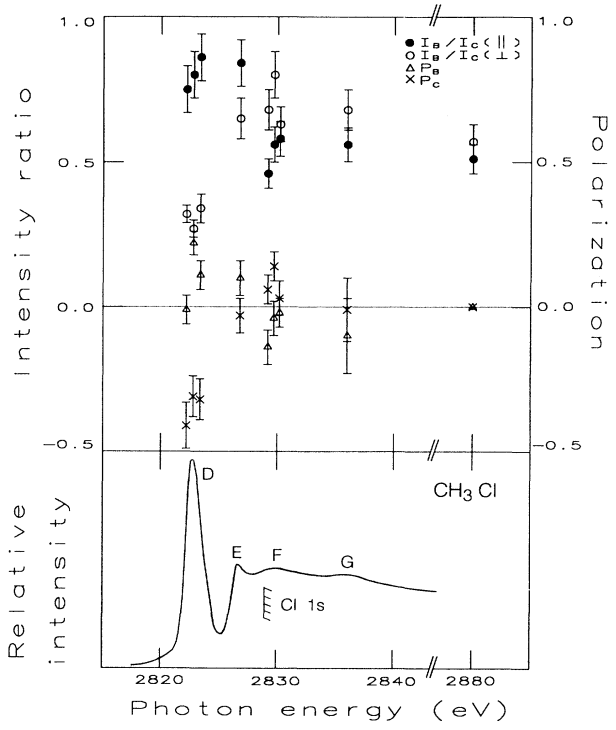

FIG. 4. Measured B-to-C K-V peak-intensity ratios for CH_3Cl as a function of incident photon energy and x-ray polarization angle, and derived polarization values P for K-V peaks B and C. The absorption spectrum is reproduced for comparison.

These values are shown in Table II and plotted in Fig. 4. The large polarization effect for feature-D excitation is readily apparent, as are possible smaller effects at features E, F, and G. Differences in parallel and perpendicular ratios of 0.1 or less are not considered significant, although the general trend for above-threshold energies might suggest a bigger B-to-C ratio for perpendicular polarization.

At the highest photon energy studied, 2880 eV, the B-to-C ratios for the two polarization angles are identical to within experimental uncertainty. This indicates that the values for P for peaks B and C are essentially equal at 2880 eV. Exact equality of P values is possible only for $P_B=P_C=0$, and thus $a_\parallel=a_\perp$, and the ionization process well above threshold should be isotropic. It is useful to realize that polarization effects above the ionization threshold will reflect alignment of the K-hole state, just as for resonant excitation (e.g., on feature D). Alignment in the above-threshold case refers to nonstatistical population of the available continuum states (ka_1, ka_2, and ke), which is expected to occur close to threshold where the continuum electron interacts most strongly with the molecular ion. Far above threshold, if ionization is atomiclike, no alignment is expected, and no polarization

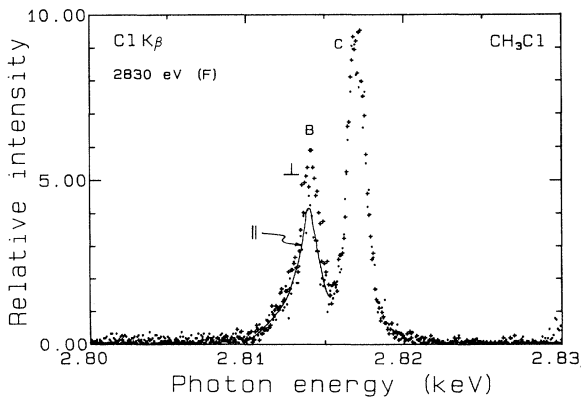

FIG. 5. Same as Fig. 3, but at 2829.7-eV excitation, on feature F of the absorption spectrum in Fig. 2.

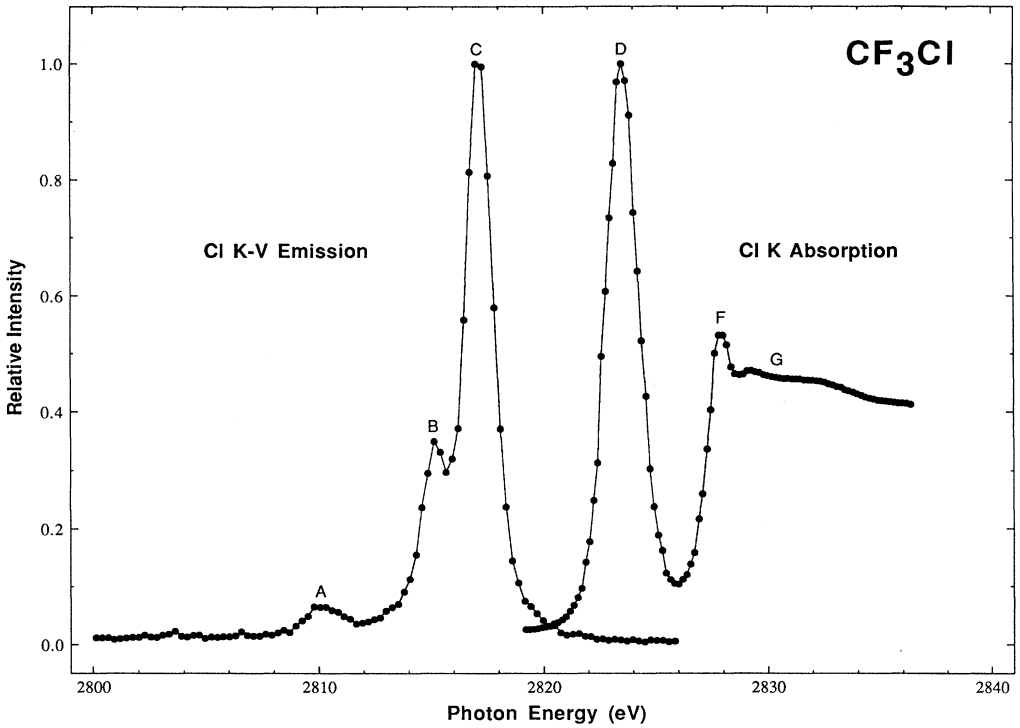

FIG. 6. Same as Fig. 2, except for CF_3Cl.

effect should be evident. More detailed measurements need to be made to fully confirm this expectation.

Assuming that 2880-eV ionization is indeed isotropic (i.e., $P_B = P_C = 0$), we can use the 2880-eV spectra as baseline measurements to determine values of P for both peaks B and C under conditions of near-threshold excitation. These results for peaks B and C are listed in Table II and plotted in Fig. 4. The P results, of course, exhibit clearly the effect of polarization for feature-D excitation. At higher energies (near features E and F), we observe small but probably significant degrees of polarization. These suggestive findings illustrate the potential of PXES for spectroscopic analysis due to its sensitivity, even in these preliminary measurements, to the near-threshold absorption structure of gas-phase molecules.

To illustrate this sensitivity more clearly, we show in Fig. 5 PXES spectra for excitation at 2829.8 eV on feature F in the CH_3Cl absorption spectrum of Fig. 2. These two parallel- and perpendicular-polarization spectra have been scaled to have identical peak-C areas, as was done for the feature-D spectra in Fig. 3. Two obvious differences with respect to Fig. 3 are notable. Firstly, the polarization effect is much smaller, but it persists even above the ionization threshold. Second, the polarization effect is reversed compared to feature-D excitation; peak B is now relatively bigger in the perpendicular-polarization spectrum. As immediate result of this latter observation is that ionization associated with feature F has a small but definite preference for producing an e-symmetry continuum channel, in contrast to feature D which is an a_1-symmetry resonance. If the suggestion[32] that F is a shape resonance is correct, then the present results imply that it is an e-symmetry shape resonance. However, preliminary indications from theoretical calculations[57] are that feature F is not a shape resonance, but is associated with a multielectron transition.

B. CF_3Cl

Figure 6 shows a measured CF_3Cl absorption spectrum in the Cl K-edge region and a Cl K-V emission spectrum taken with an incident photon energy of 2880 eV, far above the Cl 1s threshold. Peak energies and possible assignments are presented in Table III, all of which have been adopted from Refs. 13 and 58. As with CH_3Cl, feature D in absorption is of major interest, and is attributed to Cl 1s (CF_3Cl $1a_1$) excitation to the $11a_1$ anti-

TABLE III. Energies and assignments of Cl K-V x-ray emission peaks and Cl-K absorption features of CF_3Cl. Values in parentheses denote errors in the last digit(s).

Peak or feature	Energy	Assignment
A	2810.1(3)	$4e$, $9a_1 \rightarrow 1a_1$
B	2815.1(3)	$10a_1$, $5e \rightarrow 1a_1$
C	2817.1(3)	$7e \rightarrow 1a_1$
D	2823.5[a]	$1a_1 \rightarrow 11a_1$
F	2827.8(3)	$1a_1 \rightarrow 4p$ Rydberg
G	2829.2(3)	$1a_1 \rightarrow np$ Rydberg
Cl K IP	2830.2(3)	threshold

[a]LaVilla (Ref. 58).

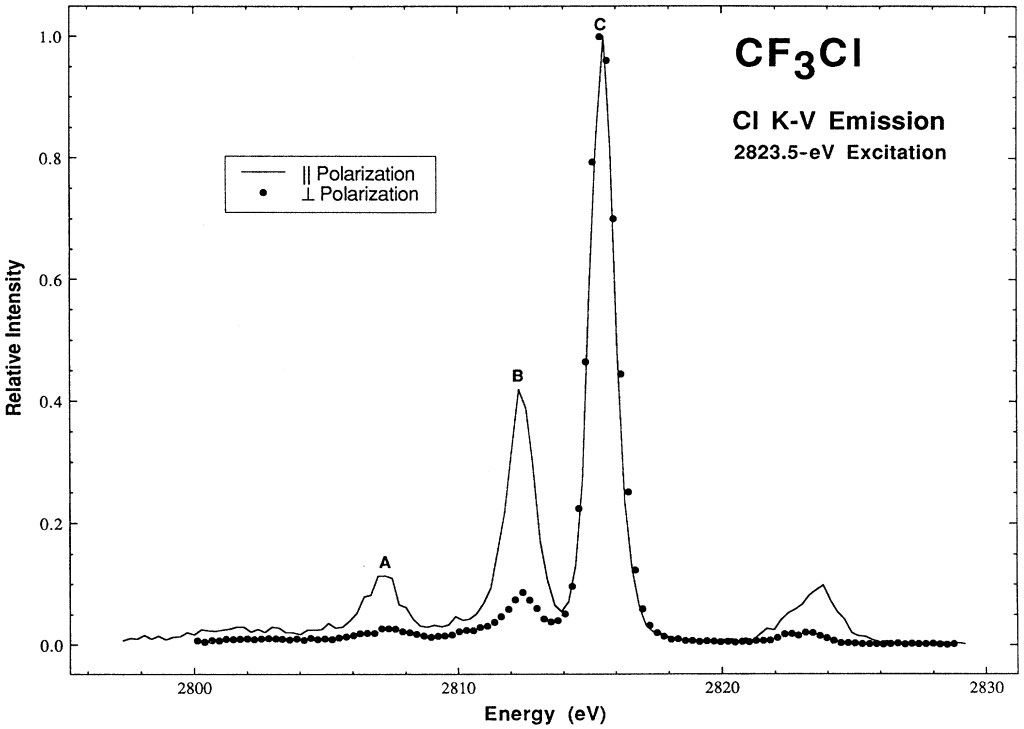

FIG. 7. Same as Fig. 3, except for CF_3Cl at 2823.5-eV excitation.

bonding MO. For the *K-V* emission spectrum in Fig. 6, the important occupied MO's are the $7e$, $10a_1$, $5e$, $9a_1$, and $4e$, due to their partial Cl $3p$ character. They contribute to the *K-V* peaks *C* ($7e$), *B* ($10a_1$ and $5e$), and *A* ($9a_1$ and $4e$), respectively.

The absolute energy scale for Fig. 6 and Table III was established in a manner identical to that described for CH_3Cl. (This is also true for $CFCl_3$ and CF_2Cl_2.) The absorption-feature *D* energy (2823.5 eV) was provided by LaVilla,[58] and the Cl $1s$ binding energy [2830.2(3) eV] was obtained using our measured *K-V* energies and valence electron binding energies.[42,54,59–65]

Turning the primary monochromator energy to 2823.5 eV, right on absorption feature *D*, the PXES spectra of CF_3Cl in Fig. 7 were obtained. What appears to be improved resolution relative to the emission spectrum in Fig. 6 is in fact due to differential emission peak energy shifts under resonant-excitation conditions (see Refs. 7 and 8). As before, no polarization effect is detectable for 2880-eV excitation. The intensity of emission peak *C* in both spectra of Fig. 7 has been scaled equally for comparison.

Qualitatively, the PXES results in Fig. 7 can be understood by reference to the discussion for CH_3Cl, because CF_3Cl has the same symmetry, and the excitation and emission transitions are analogous to those in CH_3Cl. Likewise, quantitative interpretation using Eqs. (1) and (2) also follows directly from the discussion of CH_3Cl. Based on the *A*-to-*C* and *B*-to-*C* peak intensity ratios in both polarizations (Table IV) for feature-*D* excitation

TABLE IV. Measured Cl *K-V* peak-intensity ratios for CF_3Cl. Values in parentheses denote errors in the last digit(s).

Photon energy	*A*-to-*C* peak ratio		*B*-to-*C* peak ratio		Comments
	∥	⊥	∥	⊥	
2822.6	0.14(1)	0.04(1)	0.47(3)	0.10(1)	
2823.5	0.18(2)	0.05(1)	0.47(3)	0.10(1)	*D*
2824.4	0.20(3)	0.06(1)	0.54(6)	0.14(1)	
2824.6	0.26(2)	0.05(1)	0.69(4)	0.13(1)	
2827.8	0.09(1)	0.10(1)	0.39(2)	0.47(5)	*F*
2828.4	0.09(1)	0.10(1)	0.40(2)	0.38(2)	
2829.2	0.09(1)	0.08(1)	0.38(4)	0.29(2)	*G*
2832.4	0.10(1)	0.08(1)	0.36(2)	0.29(2)	*H*

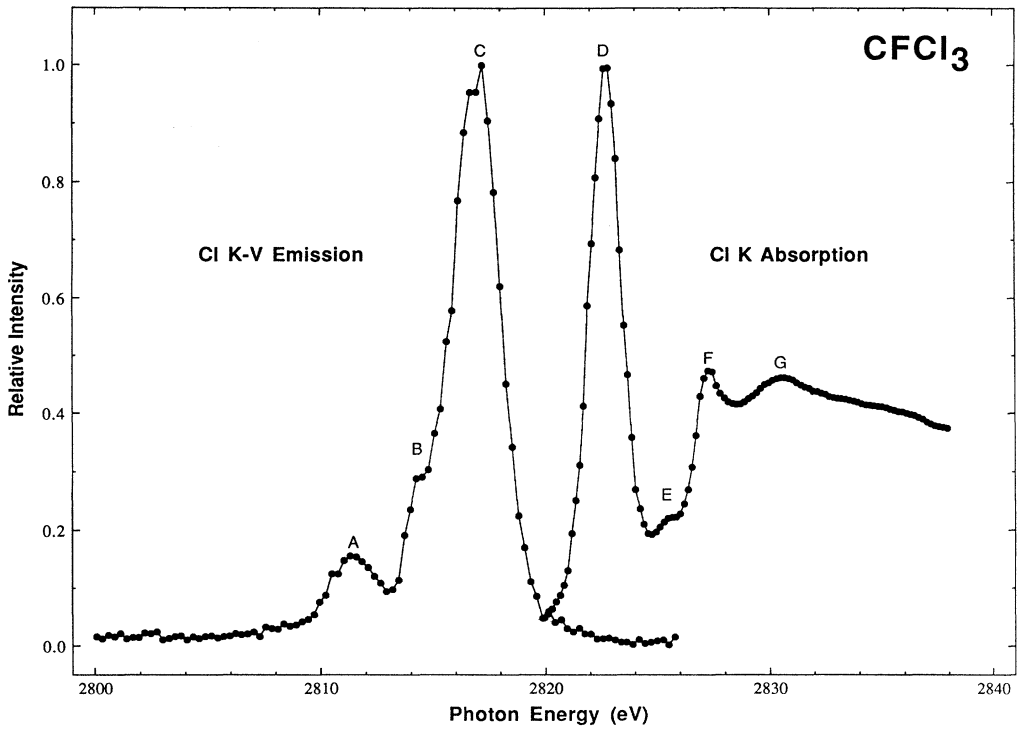

FIG. 8. Same as Fig. 2, except for $CFCl_3$.

in CF_3Cl, we can determine directly the K-V fluorescence yields $[f_{\parallel}(9a_1 \rightarrow 1a_1) + f_{\perp}(4e \rightarrow 1a_1)]$ and $[f_{\parallel}(10a_1 \rightarrow 1a_1) + f_{\perp}(5e \rightarrow 1a_1)]$ relative to $f_{\perp}(7e \rightarrow 1a_1)$. The results are 0.10(3) and 0.24(4), respectively. The present data for CF_3Cl (and $CFCl_3$ and CF_2Cl_2) are not sufficiently comprehensive to permit the polarization analysis described in Sec. III A 1.

At some incident photon energies other than 2823.5 eV (feature D), we measured A-to-C and B-to-C peak-intensity ratios as a function of polarization angle. These values are given in Table IV. Generally, we observe a polarization dependence for the ratios for incident energies near feature D in the absorption spectrum.

C. $CFCl_3$

Figure 8 shows a measured $CFCl_3$ absorption spectrum in the Cl K-edge region and a Cl K-V emission spectrum taken with an incident photon energy of 2880 eV, well above the Cl 1s threshold. Peak energies and probable assignments are given in Table V, and have been adopted from Refs. 13 and 58. Previous results[7] for Cl K-V emission disagree with the present peak energies due to calibration errors in the earlier measurement.

In contrast to CH_3Cl and CF_3Cl, $CFCl_3$ has three constituent chlorine atoms, rendering the Cl K absorption and emission processes more complicated, even though

TABLE V. Energies and assignments of Cl K-V x-ray emission peaks and Cl-K absorption features of $CFCl_3$. Values in parentheses denote errors in the last digit(s).

Peak or feature	Energy		Assignment
	This work	Ref. 7[a]	
A	2811.5(4)	2812.4	$7e \rightarrow 1a_1$, $1e$
B	2814.4(5)	2815.0	$8e \rightarrow 1a_1$, $1e$
C	2816.7(5)	2817.3	$11a_1$, $9e$, $10e$, $2a_2 \rightarrow 1a_1$, $1e$
D	2822.8[b]	2822.6	$1a_1$, $1e \rightarrow 11e$
E	2825.7(5)	2826	$1a_1$, $1e \rightarrow 12a_1$, $13a_1$
F	2827.2(3)	2827.4	$1a_1$, $1e \rightarrow 4p$ Rydberg
Cl K IP	2829.3(5)	2829.4	threshold
G	2830.0(5)	2831	

[a]Perera *et al.*
[b]LaVilla (Ref. 58).

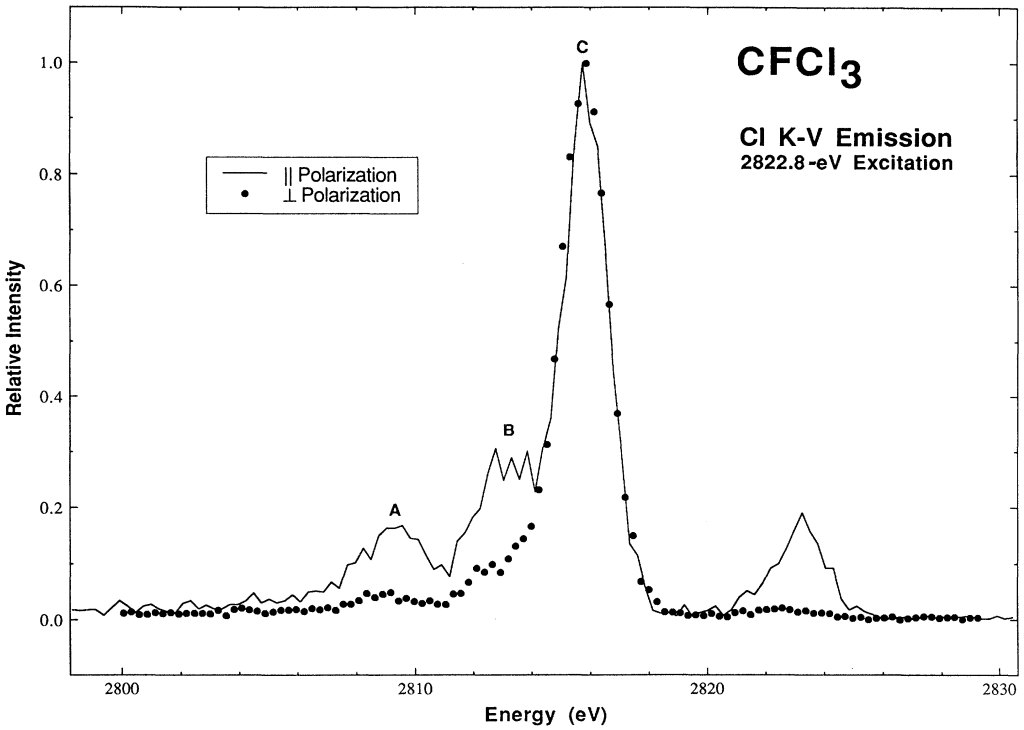

FIG. 9. Same as Fig. 3, except for $CFCl_3$ at 2822.8-eV excitation.

adherence to C_{3v} symmetry is maintained. For instance, the six Cl 1*s* electrons reside in the $1a_1$ and $1e$ molecular core orbitals, which are nearly degenerate and unresolvable due to the large core-hole lifetime width. Furthermore, the $1a_1$ and $1e$ orbitals have orthogonal transition moments to any one valence MO. The presence of three chlorine atoms also triples the population of Cl 3*p* electrons, increasing the number of valence MO's available to interact with the Cl 1*s* hole by radiative decay. These added complications are reflected in the assignments of Table V, in which, for example, the main *K-V* emission peak (*C*) for $CFCl_3$ receives contributions from five different valence orbitals, all of Cl lone-pair character.

The absolute energy scale for the $CFCl_3$ results was established as for CF_3Cl, with the energy of absorption feature *D* (2822.8) provided by Ref. 58. Previous measurements[42,48,54,59,62,63] were used to help determine the Cl 1*s* IP to be 2829.3(5) eV.

Figure 9 shows the PXES results for 2822.8-eV excitation on absorption feature *D* in Fig. 8. No polarization effect was observed for 2880-eV excitation. The rather dramatic polarization effect for resonance excitation at 2822.8 eV may seem quite surprising because of the complicated nature of the peak assignments. Both emission peaks *A* and *B* essentially disappear in perpendicular polarization. However, recourse to Eqs. (1) and (2), which is applicable to $CFCl_3$ if localization of the Cl(1*s*) hole on a particular Cl atom is unimportant, provides a qualitative explanation. First, a given absorption and/or emission process starts either from the $1a_1$ or the $1e$ Cl 1*s* orbital, not both simultaneously. Because these two initial orbitals have different symmetries, we must consider their contributions separately to the PXES results. For example, the $1e \rightarrow 11e$ absorption transition is parallel to the molecular symmetry axis (along the C—F bond), and thus excited molecules will be aligned preferentially parallel to the SR polarization. Similarly, for example, the emission transition $8e \rightarrow 1e$, which contributes to peak *B* (and which follows the $1e \rightarrow 11e$ excitation), is polarized parallel to the symmetry axis, and will emit x rays polarized parallel to the SR polarization. An analogous argument can be made for the other contribution to peak *B*; namely, $1a_1 \rightarrow 11e$ excitation, followed by $8e \rightarrow 1a_1$ emission, with the result that all contributions to emission peak *B* (and similarly peak *A*) should be strongly polarized parallel to the SR polarization, as we observe.

Two aspects related to the discussion of peak-*B* emission illustrate the spectroscopic usefulness of PXES. First, a significant contribution to absorption feature *D* by the $1a_1$, $1e \rightarrow 12a_1$ transitions can be tentatively ruled out, because it would cause emission peak *B* to exhibit some degree of perpendicular polarization, contrary to observation. Second, we can also rule out any significant contribution to emission peak *A* from the $10a_1$ valence MO, because it would render peak *A* partially perpendicularly polarized. This latter result is consistent with estimated intensities from Ref. 13, where the $7e$ valence MO is expected to be more important for peak *A* emission. Finally, for emission peak *C*, little can be deduced at this time due to the number of possible contributions

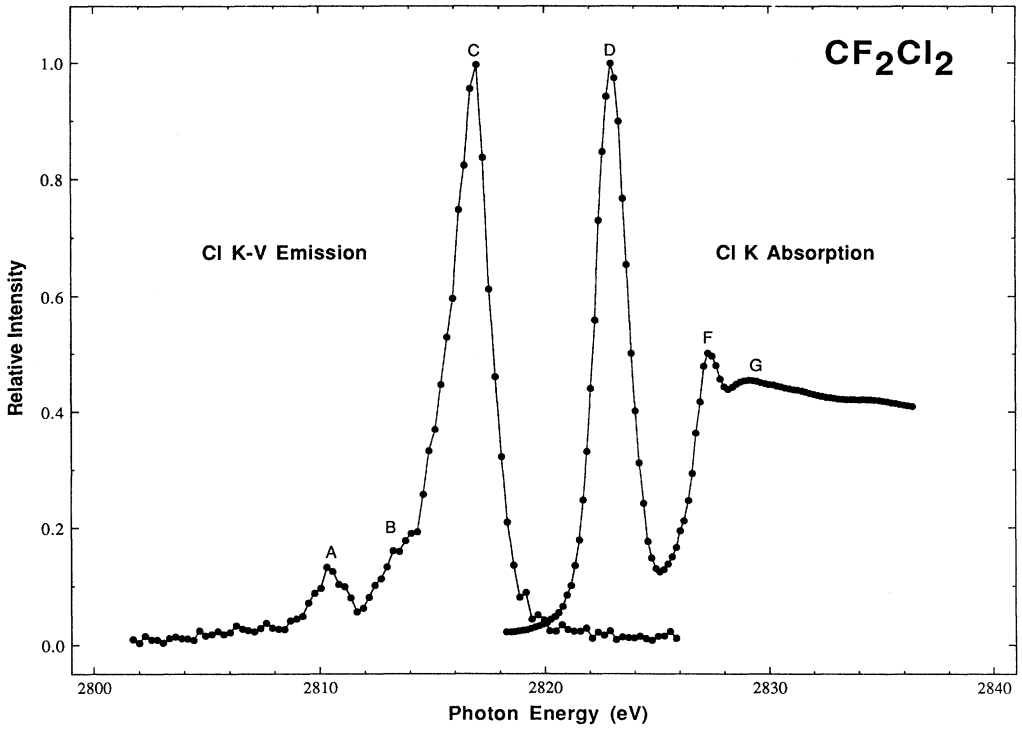

FIG. 10. Same as Fig. 2, except for CF_2Cl_2.

to this peak. Further experimental and theoretical work is required.

D. CF_2Cl_2

Figure 10 shows a measured CF_2Cl_2 absorption spectrum in the Cl *K*-edge region and a Cl *K-V* emission spectrum taken with an incident photon energy of 2880 eV, well above the Cl 1*s* threshold. Peak energies and possible assignments are listed in Table VI. The energies are based on Ref. 58, and the assignments are from Ref. 57. Because of its C_{2v} symmetry, CF_2Cl_2 is qualitatively different from the other three molecules studied. The lowering of symmetry results in more valence MO's contributing to the *K* absorption and *K-V* emission spectra, as evidenced in the assignments in Table VI. Nevertheless, a definite polarization effect is observed (Fig. 11) for excitation at 2823.0 eV on feature *D* in the absorption spectrum of Fig. 10. As before, the absolute energy scale for the data in Figs. 10 and 11 and in Table VI has been established by fixing the energy of absorption feature *D* based on previous work,[58] and using measured valence MO binding energies[42,48,54,57,62,63,66] to estimate the Cl 1*s* IP to be 2829.6(6) eV. Because of the complicated nature of the *K-V* spectra and the paucity of experimental data, no further interpretation is possible at this time.

TABLE VI. Energies and assignments of Cl *K-V* x-ray emission peaks and Cl-*K* absorption features of CF_2Cl_2. Values in parentheses denote errors in the last digit(s).

Peak or feature	Energy		Assignment
	This work	Ref. 34[a]	
A	2810.4(3)		$10a_1$, $4b_1$, $6b_2 \rightarrow 1a_1$, $1b_2$
B	2813.1(5)		$11a_1$, $2a_2 \rightarrow 1a_1$, $1b_2$
C	2816.5(4)		$12a_1$, $3a_2$, $6b_1$, $7b_2$, $8b_2 \rightarrow 1a_1$, $1b_2$
D	2823.0[b]	2823.1	$1a_1$, $1b_2 \rightarrow 13a_1$, $9b_2$
F	2827.2(3)	2827.6	$1a_1$, $1b_2 \rightarrow 4p$ Rydberg
G	2829.1(4)		$1a_1$, $1b_2 \rightarrow np$ Rydberg
Cl *K* IP	2829.6(6)		threshold

[a]Hanus and Gilberg.
[b]LaVilla (Ref. 58).

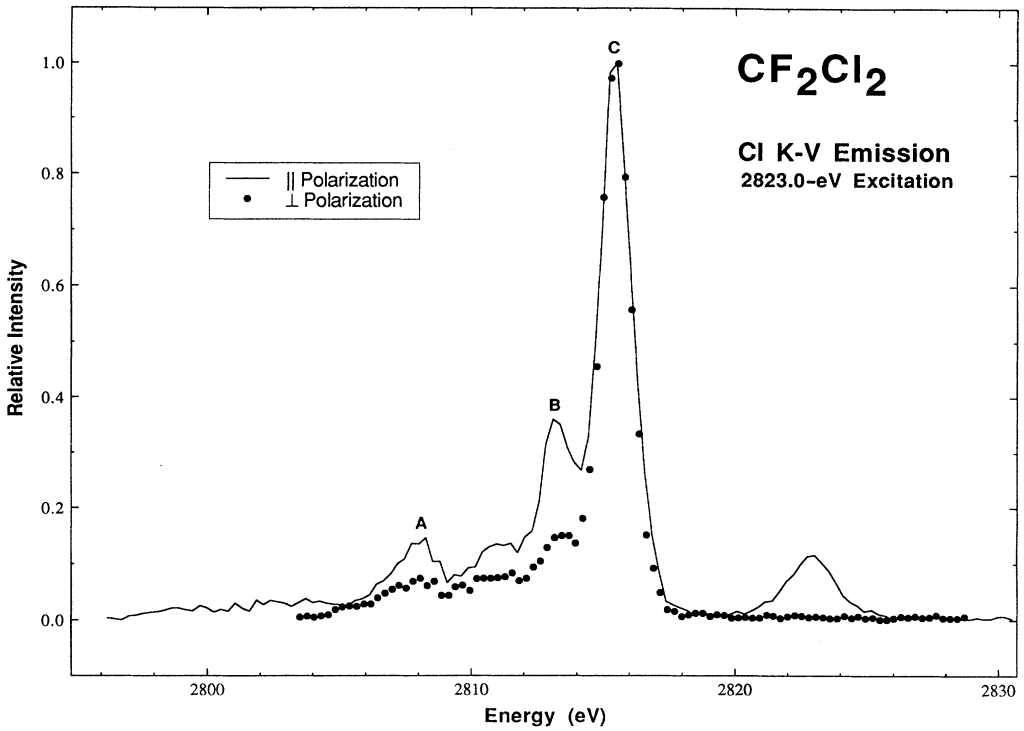

FIG. 11. Same as Fig. 3, except for CF_2Cl_2 at 2823.0-eV excitation.

IV. CONCLUDING REMARKS

Results on small chlorine-containing molecules have been used to demonstrate polarized x-ray-emission spectroscopy (PXES). Observations indicate that the degree and the direction of x-ray polarization is sensitive to the initial excitation energy in the core-level region, and to the symmetry properties of the valence molecular orbital(s) involved in the x-ray-emission process. Qualitatively, PXES has been used to study the symmetry of occupied and unoccupied orbitals in free molecules by observing the direction of x-ray-emission polarization. Quantitative interpretation requires in addition the use of a classical theoretical model. For spectroscopically complicated systems (e.g., $CFCl_3$), a polarization effect is observable, which suggests that PXES may be applicable to selected larger and more complicated systems, such as larger molecules, adsorbates, solids and interfaces, and liquid solutions. Further experimental work clearly is indicated to bring these possibilities to fruition.

ACKNOWLEDGMENTS

The authors are grateful to J. A. Sheehy and P. W. Langhoff for helpful discussions, to P. Indelicato and A. Henins for help in measuring the absolute efficiency of the secondary spectrometer, to D. J. Berkeland for assistance in the data analysis, and to B. A. Karlin for assistance with the experiment. The experiments were performed at the National Synchrotron Light Source, which is supported by the U.S. Department of Energy under Contract No. DE-AC020-76CH00016. One of us (R.C.C.P.) acknowledges support by the U.S. Department of Energy under Contract No. DE-AC03-76SF00098.

[1]A. Meisel, G. Leonhardt, and R. Szargan, *Röntgenspectren und Chemische Bindung* (Akademische Verlagsgesellschaft, Leipzig, 1977).

[2]R. E. LaVilla, in *Advances in X-ray Spectrosocopy,* edited by C. Bonnelle and C. Mande (Pergamon, New York, 1982).

[3]R. D. Deslattes, Aust. J. Phys. **39**, 845 (1986).

[4]H. Winick, in *Synchrotron Radiation Research,* edited by H. Winick and S. Doniach (Plenum, New York, 1980).

[5]R. D. Deslattes, R. E. LaVilla, P. L. Cowan, and A. Henins, Phys. Rev. A **27**, 923 (1983).

[6]P. L. Cowan, S. Brennan, R. D. Deslattes, A. Henins, T. Jach, and E. G. Kessler, Nucl. Instrum. Methods **246**, 154 (1986); P. L. Cowan, S. Brennan, T. Jach, D. W. Lindle, and B. A. Karlin, Rev. Sci. Instrum. **60**, 1603 (1989).

[7]R. C. C. Perera, R. E. LaVilla, P. L. Cowan, T. Jach, and B. Karlin, Phys. Scr. **36**, 132 (1987).

[8]R. C. C. Perera, P. L. Cowan, D. W. Lindle, and R. E. LaVilla J. Phys. (Paris) Colloq. **48**, C9-753 (1987).

[9]D. W. Lindle, P. L. Cowan, R. E. LaVilla, T. Jach, R. D. Deslattes, R. C. C. Perera, and B. Karlin, J. Phys. (Paris) Colloq. **48**, C9-761 (1987).

[10]D. W. Lindle, P. L. Cowan, R. E. LaVilla, T. Jach, R. D.

Deslattes, B. Karlin, J. A. Sheehy, T. J. Gil, and P. W. Langhoff, Phys. Rev. Lett. **60**, 1010 (1988).
[11]D. W. Lindle, P. L. Cowan, R. E. LaVilla, T. Jach, R. D. Deslattes, R. C. C. Perera, and B. Karlin, Proc. SPIE **911**, 54 (1988).
[12]D. W. Lindle, P. L. Cowan, T. Jach, R. E. LaVilla, and R. D. Deslattes, Nucl. Instrum. Methods B **40/41**, 257 (1989).
[13]R. C. C. Perera, P. L. Cowan, D. W. Lindle, R. E. LaVilla, T. Jach, and R. D. Deslattes (unpublished).
[14]F. Kh. Gelmukhanov and L. N. Mazalov, Opt. Spektrosk. **42**, 651 (1977) [Opt. Spectrosc. (USSR) **42**, 371 (1977)].
[15]A. Faessler, E. Gilberg, and G. Weich, in *Advances in X-Ray Spectroscopy,* edited by C. Bonnelle and C. Mande (Pergamon, New York, 1982).
[16]W. Czolbe, G. Dräger, O. Brümmer, and A. Simunek, in *Proceedings of the X-84 International Conference on X-Ray and Inner-Shell Processes,* edited by A. Meisel and J. Finster (Karl Marx University, Leipzig, 1984), p. 103.
[17]J. Drahokoupil, A. Simunek, W. Czolbe, E. Schulz, G. Dräger, and O. Brümmer, Ref. 16, p. 125.
[18]G. Dräger and O. Brümmer, Phys. Status Solidi B **124**, 11 (1984).
[19]G. Dräger, W. Czolbe, E. Schulz, A. Simunek, J. Drahokoupil, Y. N. Kucherenko, and V. V. Nemoshkalenko, Phys. Status Solidi B **131**, 193 (1985).
[20]G. Dräger, W. Czolbe, A. Simunek, and F. Levy, Cryst. Res. Technol. **20**, 1451 (1985).
[21]A. Simunek, G. Dräger, W. Czolbe, O. Brümmer, and F. Levy, J. Phys. Chem. **18**, 1605 (1985).
[22]G. Dräger and O. Brümmer, in *Proceedings of the X-84 International Conference on X-Ray and Inner-Shell Processes,* edited by A. Meisel and J. Finster (Karl Marx University, Leipzig, 1984), p. 337.
[23]A. Simunek, Ref. 22, p. 440.
[24]J. Hrdy, A. Henins, and J. A. Bearden, Phys. Rev. A **2**, 1708 (1970).
[25]See, for example, E. D. Poliakoff, J. L. Dehmer, D. Dill, A. C. Parr, K. H. Jackson, and R. N. Zare, Phys. Rev. Lett. **46**, 907 (1981); E. D. Poliakoff, J. L. Dehmer, A. C. Parr, and G. E. Leroi, J. Chem. Phys. **77**, 5243 (1982); J. W. Keller, W. T. Hill III, D. L. Ederer, T. J. Gil, and P. W. Langhoff, *ibid.* **87**, 3299 (1987).
[26]S. Brennan, P. L. Cowan, R. D. Deslattes, A. Henins, D. W. Lindle, and B. A. Karlin, Rev. Sci. Instrum. **60**, 2243 (1989).
[27]H. F. Beyer and D. Leisen, Nucl. Instrum. Methods A **272**, 895 (1988).
[28]A. Henins, Rev. Sci. Instrum. **58**, 1173 (1987).
[29]B. P. Duval, J. Barth, R. D. Deslattes, A. Henins, and G. G. Luther, Nucl. Instrum. Methods **222**, 274 (1984).
[30]We represent the x-ray fluorescence transitions using a notation borrowed from Auger spectroscopy. For example, *K-V* refers to x-ray fluorescence that occurs when a valence (*V*) electron fills a 1*s* (*K*) vacancy. Generalization to multiple-hole or multiple-electron transitions is straightforward.
[31]R. D. Deslattes and R. E. LaVilla, Appl. Opt. **6**, 39 (1967).
[32]R. C. C. Perera, J. Barth, R. E. LaVilla, R. D. Deslattes, and A. Henins, Phys. Rev. A **32**, 1489 (1985).
[33]E. Gilberg, Z. Phys, **236**, 21 (1970).
[34]M. J. Hanus and E. Gilberg, J. Phys. B **9**, 137 (1976).
[35]F. P. Larkins and R. A. Phillips, J. Chem. Phys. **88**, 5323 (1988).
[36]R. E. LaVilla and R. D. Deslattes, J. Chem. Phys. **45**, 3446 (1966).
[37]V. I. Nefedov, J. Struct. Chem. **12**, 276 (1971).
[38]R. C. C. Perera, R. E. LaVilla, and G. V. Gibbs, J. Chem. Phys. **86**, 4824 (1987).
[39]A. P. Hitchcock and C. E. Brion, J. Electron Spectrosc. **14**, 417 (1978).
[40]A. P. Hitchcock and C. E. Brion, J. Electron Spectrosc. **17**, 139 (1979).
[41]S. M. Blokhin, A. P. Sadovskii, G. N. Dolenko, and V. M. Bertenev, J. Struct. Chem. **10**, 722 (1969).
[42]D. W. Turner, C. Baker, A. D. Baker, and C. R. Brundle, *Molecular Photoelectron Spectroscopy* (Wiley-Interscience, London, 1970).
[43]A. W. Potts, H. J. Lempka, D. G. Streets, and W. C. Price, Philos. Trans. R. Soc. London Ser. A **268**, 59 (1970).
[44]J. L. Ragle, I. A. Stenhouse, D. C. Frost, and C. A. McDowell, J. Chem. Phys. **53**, 178 (1970).
[45]F. Hopfgarten and R. Manne, J. Electron Spectrosc. **2**, 13 (1973).
[46]L. Karlsson, R. Jadrny, L. Mattsson, F. T. Chau, and K. Siegbahn, Phys. Scr. **16**, 225 (1977).
[47]A. P. Hitchcock and C. E. Brion, J. Electron Spectrosc. **13**, 193 (1978).
[48]C. E. Brion, W. B. Stewart, D. S. C. Lee, and P. Crowley, J. Electron Spectrosc. **23**, 399 (1981).
[49]D. Li, J.-K. Zhu, J. Li, and Y.-K. Pan, Chem. Phys. Lett. **87**, 463 (1982).
[50]W. Von Niessen, L. Åsbrink, and G. Bieri, J. Electron Spectrosc. **26**, 173 (1982).
[51]P. R. Keller, J. W. Taylor, T. A. Carlson, and F. A. Grimm, Chem. Phys. **79**, 269 (1983).
[52]I. Novak, J. M. Benson, and A. W. Potts, J. Electron Spectrosc. **41**, 225 (1986).
[53]E. P. Bertin, in *Handbook of Spectroscopy,* edited by J. W. Robinson (CRC, Cleveland, 1974) Vol. 1, p. 238.
[54]K. Watanabe, T. Nakayama, and J. Mottl, J. Quant. Spectrosc. Rad. Transfer **2**, 369 (1962).
[55]E. D. Poliakoff, L. A. Kelly, L. M. Duffy, B. Space, P. Roy, S. H. Southworth, and M. G. White, J. Chem. Phys. **89**, 4048 (1988); Chem. Phys. **129**, 65 (1989).
[56]T. X. Carroll and T. D. Thomas, J. Chem. Phys. **89**, 5983 (1988), and references therein.
[57]P. W. Langhoff and J. A. Sheehy (private communication).
[58]R. E. LaVilla (unpublished results).
[59]J. Doucet, P. Sauvageau, and C. Sandorfy, J. Chem. Phys. **58**, 3708 (1973).
[60]R. Gilbert, P. Sauvageau, and C. Sandorfy, J. Chem. Phys. **60**, 4820 (1974).
[61]H. W. Jochims, W. Lohr, and H. Baumgärtel, Ber. Bunsenges. Phys. Chem. **80**, 130 (1976).
[62]T. Cvitas, H. Güsten, and L. Klasinc, J. Chem. Phys. **67**, 2687 (1977).
[63]R. Jadrny, L. Karlsson, L. Mattsson, and K. Siegbahn, Phys. Scr. **16**, 235 (1977).
[64]A. W. Potts, I. Novak, F. Quinn, G. V. Marr, B. Dobson, I. H. Hillier, and J. B. West, J. Phys. B **18**, 3177 (1985).
[65]F. T. Chau and C. A. McDowell, J. Electron Spectrosc. **6**, 357 (1975).
[66]J. C. Bunzli, D. C. Frost, F. G. Herring, and C. A. McDowell, J. Electron Spectrosc. **9**, 289 (1976).